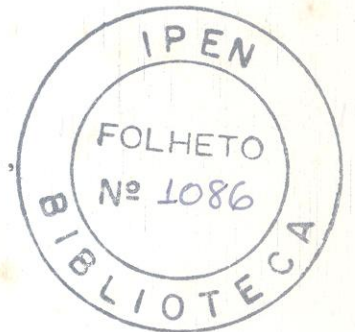


8.6. THE INFLUENCE OF NIOBIUM ON THE OXIDATION OF ALL-AUSTENITE STAINLESS STEELS

Lalgudi V. Ramanathan and Angelo F. Padilha,
 Instituto de Pesquisas Energeticas e Nucleares,
 São Paulo, Brazil.



ABSTRACT

The influence of niobium content (0.5-2.0wt%) on the oxidation behavior of Fe-15%Cr-15%Ni austenitic stainless steel has been studied by isothermal and cyclic oxidation tests in air at different temperatures in the range 800-1200°C. The isothermal oxidation rate, the scaling index and the cumulative oxide loss decreased with increasing niobium content. X-ray diffraction and fluorescence analysis of detached oxide scales revealed that the niobium in the alloy matrix facilitated the formation of Cr_2O_3 near the metal-metal oxide boundary, which decreased further oxidation. S.E.M./EDAX observations revealed that external Fe_2O_3 morphology changed from being nodular to needlelike with 2% increase in niobium content.

INTRODUCTION

Niobium stabilized stainless steels have been used in both normal and high temperature service environments. The niobium in these steels is usually present in the form of carbides, and it can also

accentuate the formation of δ -ferrite, deformation induced martensites and the precipitation of Laves phase Fe_2Nb . The influence of niobium on the oxidation behavior of stainless steels is as yet not clear. Mangone et al [1] reported that the addition of 2% niobium reduced oxidation resistance of cast stainless steels. On the other hand, Truman and Pirt [2] reported that the addition of 0.77% niobium to 18%Cr-10%Ni stainless steels did not cause any significant changes in the high temperature oxidation behavior. Recently Suzuki and Kawabata [3] found that austenitic stainless steels with small quantities of niobium showed improved resistance to cyclic oxidation behavior in air between 800 and 1200°C. In all these investigations as well as in others [4,5], where in the oxidation behavior of niobium stabilized austenitic stainless steels of the 300 series have been studied, the niobium is generally present as carbides. It is well known that the high temperature oxidation behavior of stainless steels is influenced by the nature of the matrix, (ferritic or austenitic) [6], alloying or

'tramp' elements, intermetallic phases, and precipitates present in the steel.[7,8] Also, since the niobium added to the stainless steels could be present in the form of one or more phases, in this investigation, the influence of niobium addition and not that of the phases precipitated by niobium addition on the oxidation behavior of austenitic stainless steels has been studied. To do this, a base matrix consisting of Fe-15%Cr-15%Ni was selected and 0.5%, 1% and 2% niobium added. A low carbon content and a high solubilization temperature helped maintain almost all the niobium dissolved in the matrix.

EXPERIMENTAL

The alloys containing the different niobium contents (and as shown in Table I) were produced by vacuum melting from high purity starting materials. As mentioned earlier, the carbon level was maintained low to minimize niobium consumption. The

Table I. Chemical analysis of alloys.

ELEMENT	ALLOY			
	A	B	C	D
C	0.040	0.038	0.029	0.033
Si	0.79	0.62	0.66	0.71
Mn	0.51	0.39	0.51	0.47
P	0.01	0.01	0.01	0.01
S	0.02	0.02	0.02	0.02
Cr	14.2	14.3	14.9	14.1
Ni	14.6	14.6	13.9	14.8
Nb	-	0.44	0.94	1.90

alloys were subsequently forged, heat-treated and machined to give specimens (a) 5mm in diameter and 1mm thick for

oxidation measurements in the thermogravimetric analyzer and (b) 15mm in diameter and 3mm high for the cyclic oxidation tests.

Thermogravimetric analysis

Both constant rate heating tests up to 1000 C and isothermal oxidation tests at 800° and 900° C were carried out with a Dupont thermogravimetric analyzer. The weight gain was continuously plotted as a function of temperature and/or time for the four alloys.

Cyclic oxidation tests

A 50mm diameter alumina tube test chamber was used in conjunction with a horizontal furnace to carry out the cyclic oxidation tests. The specimens were positioned within the tube in open alumina boats after the test temperature was stabilized. Each cycle was for six hours, after which the specimens were removed from the test chamber, cooled in a closed container to permit the collection of any oxide scale that might have spalled, weighed together with any spalled oxide, scrubbed with a stiff steel brush to remove any loosely adhering oxide and reweighed to give the starting weight for the next cycle. The whole procedure was repeated six times. The scaling index was considered to be the total gain in weight per unit area after six cycles. The tests were carried out in quadruplicate with each of the alloys at 800° C, 900° C, 1000° C, 1100° C and 1200° C. The difference in the weights of the specimen, before and after brushing were also recorded for each cycle to provide a measure of the quantity of scale shed.

X-ray analyses

X-ray fluorescence analyses were performed on spalled oxide specimens, both on the metal/metal oxide interface side and on the metal oxide/air interface side in a spectrometer with a rhodium target and a LiF(200) crystal analyzer. X-ray diffraction analysis of the spalled oxide from the different alloys oxidized at 1200°C for 3 hours was performed with a Rigako-Denki x-ray diffractometer using chromium K α x-rays and a vanadium filter.

Scanning electron microscopy

The surface topography and structure of detached oxides as well as oxides in-situ were examined using conventional optical microscopes and a Cambridge Stereoscan coupled to an energy dispersive analyzer.

RESULTS

Isothermal oxidation

Figure 1. shows the weight gain curves as a function of temperature for alloys A,B,C and D. It can be seen that with increasing temperature, the weight gain increases gradually at first and later on at an increased rate. The slope can be seen to change at around 500-600°C and may be attributed to increased mobility of the cation species within the oxide as well as to a change in the composition of the oxide [9].

During isothermal oxidation, the different alloys gained weight rapidly up to about 60-80 minutes, after which the rate of weight gain decreased as shown in figure 2. No breakaway oxidation was obser-

ved and the oxide layer was dark and protective. The curves in figure 2. reveal that all the alloys exhibit a near parabolic behavior with time. The overall extent of oxidation in 400 minutes increases with temperature and at either temperature, decreases with increasing niobium content.

Cyclic oxidation

Progressive weight gain versus number of cycles is shown in figure 3. The weight gain at 800°C was very low and the oxide loss from spontaneous spalling within the furnace at 1200°C too high to permit these data to be shown in figure 3. The weight gain or scaling index increases with temperature and decreases with increasing niobium content. A critical temperature is observed below which the oxide formed is protective and is not shed as scale. Above this critical temperature, oxidation rate was high and scale shedding substantial as well as roughly proportional to weight gain. The transition from low weight gain values to high weight gain values for the four alloys is quite sharp as can be observed from figure 4. The temperature at which the slope changes can be seen to increase with the niobium content of the stainless steel.

The plots of cumulative weight loss versus the number of cycles are shown in figure 5(a-d). The weight loss was calculated from the detached scale and that removed by brushing the specimens between successive cycles. Since scale was lost during or after cooling, the plots are shown in stepwise form. It can be observed that at 800°C the weight loss is quite low. At 900°C, the oxide loss commences

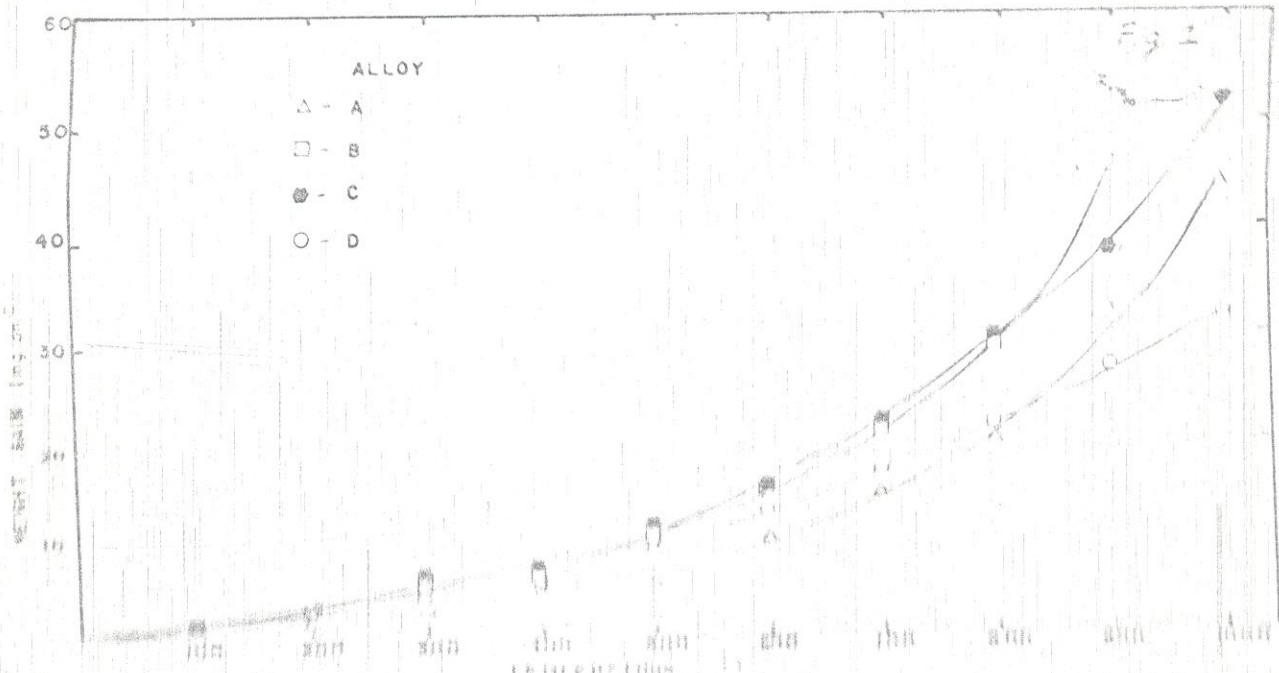


Figure 1: Relationship between alloy type and measured property.

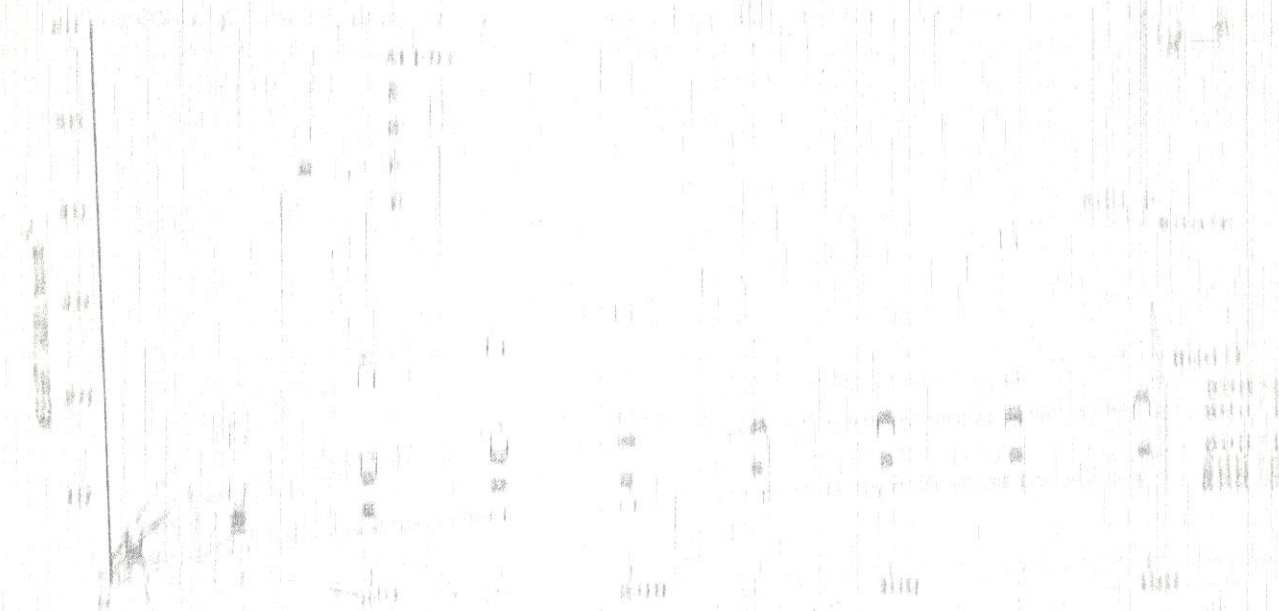


Figure 2: Comparison of alloy types across different categories.

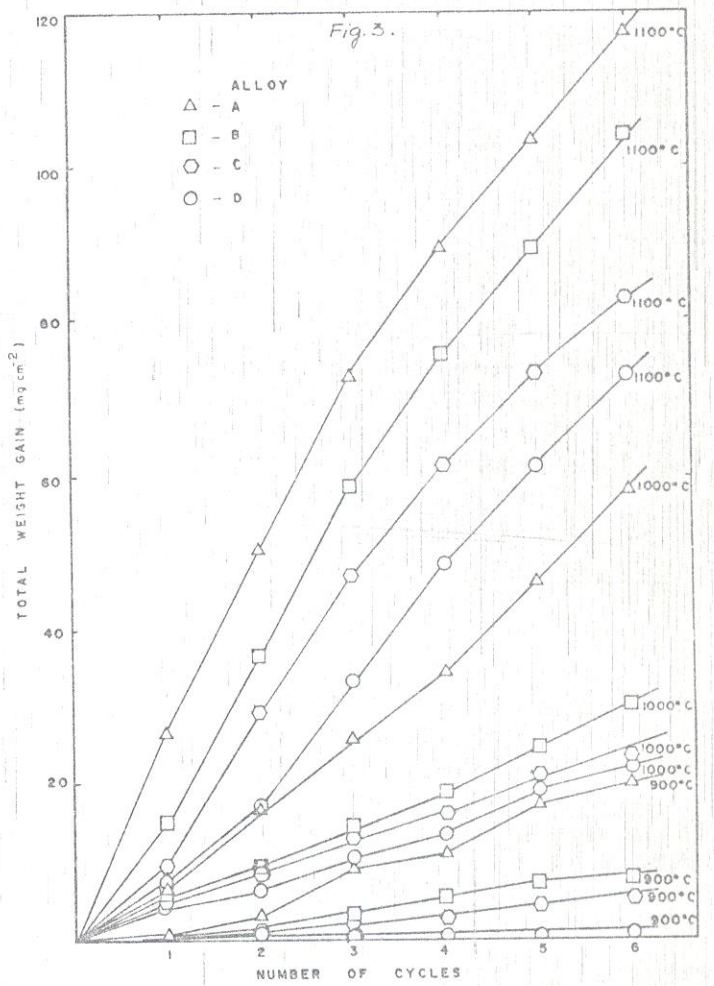


Figure 3. Weight gain versus number of six hour test cycles for alloys A,B,C and D.

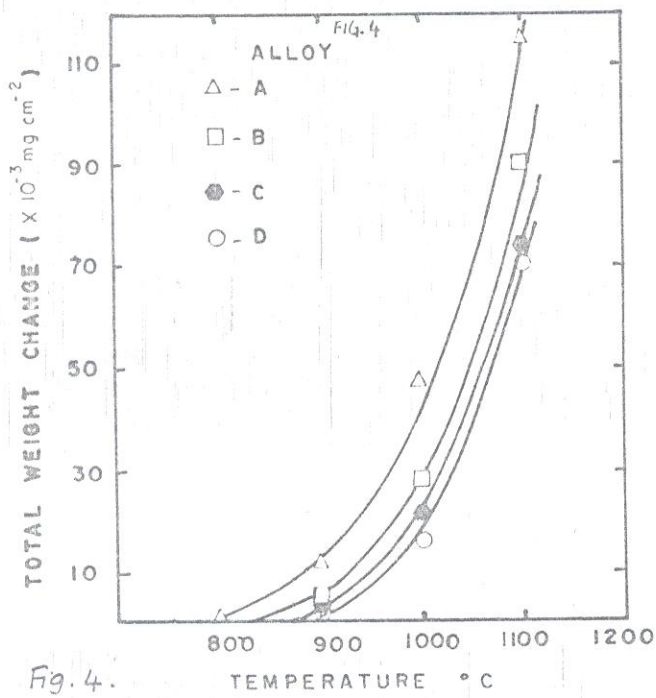
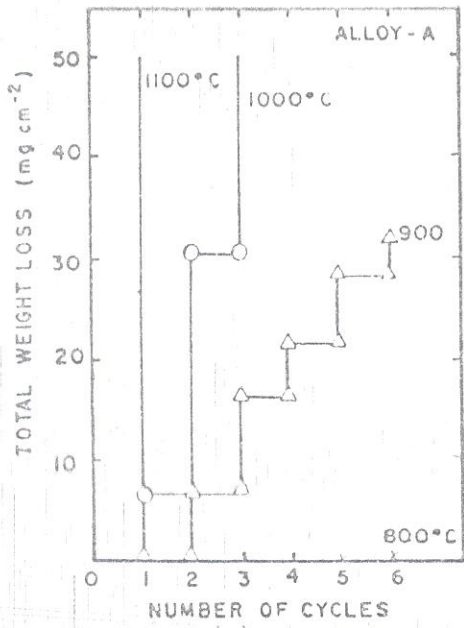
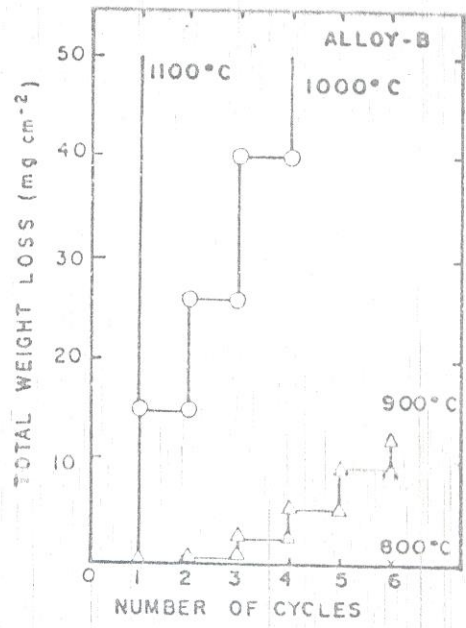


Fig. 4.

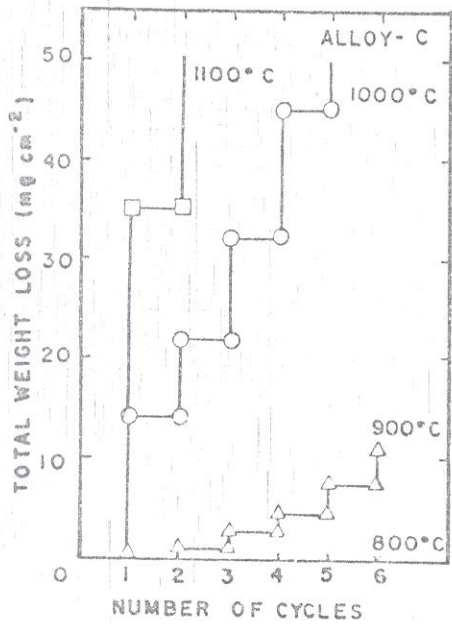
Figure 4. Weight gain versus test temperature for alloys A,B,C and D.



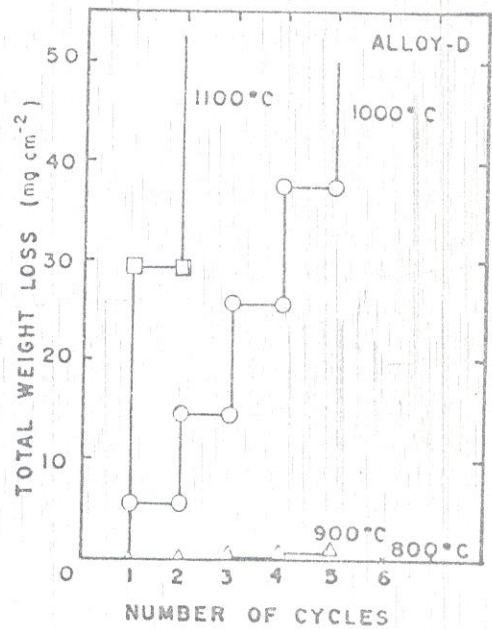
(a)



(b)



(c)



(d)

Figure 5. Total weight loss following cooling versus number of six hour test cycles: (a) alloy A, (b) alloy B, (c) alloy C and (d) alloy D.

only after the second cycle for the alloys A, B and C and decreases sharply with increasing niobium content. A similar behavior of decreasing oxide loss with increasing

niobium content of the steels can be seen at 1000°C and 1100°C for specified number of cycles of heating and cooling.

Oxide analyses

Qualitative x-ray diffraction analyses of the oxides showed that the oxide formed on niobium free alloy A was almost only Fe_2O_3 with some Fe_3O_4 . The oxide formed on alloy B was also found to be mostly iron oxides, but the quantity of Fe_3O_4 was higher than that found in the oxide on alloy A. The oxide on alloy C was once again predominantly a mixture of iron oxides but with some Cr_2O_3 . The oxide on alloy D that contained 2% niobium revealed the presence of Fe_2O_3 and a considerable quantity of Cr_2O_3 . None of the oxide specimens showed the presence of nickel or niobium oxides in detectable quantities.

The results of x-ray fluorescence analyses of oxide scales stripped from the different oxidized alloys are given as number of counts per second for the four

been taken into account in the qualitative interpretation of the data given in table II. It can be seen that the oxides are primarily those of iron and contain progressively higher concentrations of chromium as well as niobium on the metal/metal oxide side of the detached scale with increasing niobium content in the alloy.

Scanning electron microscopy

Scanning electron microscopy of the oxides formed at 1200°C for 3 hours on the four alloys revealed that the morphology of the outer surface of the oxide is quite different from that on the metal/metal oxide interface side. The morphology on the metal/metal oxide interface side, shown in figure 6, was not found to differ much with increasing niobium content. The

Table II. X-ray fluorescence results expressed as counts per second.

INTERFACE	ELEMENT	ALLOY			
		A	B	C	D
Metal/ Metal oxide	Fe	10081.3	6547.6	4032.8	1839.0
	Cr	269.67	585.75	456.85	2013.42
	Ni	511.67	380.08	60.05	9.9
	Nb	--	58.7	149.5	284.2
Metal oxide/ Air	Fe	11111.5	8011.0	5191.0	5813.0
	Cr	19.9	22.78	54.6	560.03
	Ni	12.8	11.18	--	9.25
	Nb	--	--	36.4	184.95

Data obtained using a rhodium target and a $\text{LiF}(200)$ crystal analyzer.

main elements Fe, Cr, Ni and Nb on both sides of the oxide in Table II. The penetration of the x-rays into the oxides has

morphology of the outer surface of the oxide was on the other hand found to change with the niobium content of the



Figure 6. Morphology of oxide near the metal/metal oxide interface formed on alloy B. 1000X



(b) 1050X



(a) 1300X



(c) 950X

Figure 7. Morphology of external surface of oxides formed on (a) alloy A, (b) alloy B, (c) alloy C and (d) alloy D.



(d) 950X

steel as shown in figures 7a - d. The oxides on alloys A and B with 0 and 0.5% niobium were found to be rounded and nodule like, with that on alloy B being less rounded. The oxides on alloys C and D with 1% and 2% niobium however were sharp like stalagmites and randomly oriented. Energy dispersive x-ray analysis of the oxide stalagmites as well as nodules revealed that iron was the major element with traces of chromium.

DISCUSSIONS

When the all-austenite alloys A, B, C and D containing 0, 0.5%, 1% and 2% niobium are heated in air to high temperatures, they react with the oxygen in the air to form oxides. The isothermal oxide growth curves are near parabolic for the temperatures and time intervals studied. These

results are in agreement with those reported in reference [10]. The quantity and nature of the oxide layer formed on the four alloys vary with the alloy composition and the temperature. The oxidation rate changes at a critical temperature and is high but uniform beyond this temperature. Upon cooling, the thermal stresses which arise in the oxidized specimens due to differences in the thermal coefficients of expansion of the metal and the oxide, and by the thermal shock condition, cause partial or complete spalling of the protective layer. The extent of spallation also varies with alloy composition, scale thickness and scale composition. Upon increasing the niobium content of the steels, both the extent of isothermal oxidation and the scaling index (or cumulative oxide loss) decrease markedly at the different temperatures. These observations differ from those reported by others [1,2]. The differences in the influence of niobium on oxidation behavior of stainless steels may be due to (a) the addition of insufficient niobium, (b) the presence of ferrites in the matrix and (c) the presence of niobium solely as discrete carbide particles, in the stainless steels of the other investigators.

The oxides formed on the different alloys consist primarily of Fe_2O_3 , but the quantity of Fe_3O_4 and Cr_2O_3 in the oxide increase with increasing niobium content of the alloy. Similar findings of predominant Fe_2O_3 formation and the absence of NiO in the oxides formed on all-austenite Fe-14%Cr-14%Ni stainless steels oxidized in air at 900°C for 50 hours have been

reported [10]. The amount of Cr_2O_3 in the oxide increases with increasing niobium and forms preferentially near the metal/metal oxide boundary, and probably blocks further continued outward diffusion of iron ions, and thereby further oxidation.

The overall influence of niobium on the extent of oxidation of austenitic stainless steels for the time spans and the number of cycles studied is considered to be marked. It reduces oxidation rate and scaling index at high temperatures as well as raises the breakdown temperature, if the niobium is in solid solution and not as ferrites or discrete carbide particles. The role of niobium in reducing oxidation is indirect, by facilitating the formation of Cr_2O_3 at the metal/metal oxide interface boundary and effectively blocking the diffusion of iron ions.

CONCLUSIONS

1. The alloys A,B,C and D with 0,0.5, 1.0 and 2.0 wt% niobium exhibited near parabolic behavior during isothermal oxidation at 800°C and 900°C . The overall extent of oxidation at either temperature decreased with increasing niobium content.
2. The scaling index of the four alloys determined from cyclic oxidation tests increased with increasing temperature and decreased with increasing niobium content. The scale breakdown temperature shifted to around 920°C for alloy D.
3. X-ray diffraction and fluorescence analyses of detached oxides revealed that with increasing niobium content in the

steel, the composition of the oxide changes from being a mixture of Fe_2O_3 and Fe_3O_4 on alloy A to being a mixture of Fe_2O_3 and Cr_2O_3 on alloys C and D.

4. Scanning electron microscopy and energy dispersive analyses of detached oxides revealed that the morphology of the outer Fe_2O_3 surface changed from being rounded and nodulelike on niobium free alloy A to being sharp and stalagmitelike on alloy D with 2% niobium. This effect could be attributed to the suppression of oxide grain growth in the latter alloy, due primarily to the blocking effect of the inner Cr_2O_3 at the metal/metal oxide boundary.

5. The overall influence of niobium on oxidation of austenitic stainless steels is considered to be indirect. Niobium facilitates the formation of Cr_2O_3 near the metal/metal oxide interface and thus imparts a greater degree of protection to the steel from further oxidation.

REFERENCES

1. R.J. Mangone, C.J. Slunder and A.M. Hall, Summary Report, ACI Project no: 32, Battelle Memorial Institute, July 15, 1958.
2. J.E. Truman and K.R. Pirt, Br. Corros. J., 11,4,(1976),88.
3. T. Suzuki and N. Kawabata, J. Iron Steel Inst. Jpn., 63,5,(1977),681.
4. P.A. Tempest and R.K. Wild, Oxid. Met., 23,3-4,(1985),207.
5. R.C. Lobb and H.E. Evans, Corros. Sci., 24,5, (1984), 385.

6. M.Vyklicky and M.Mericka, Br. Corros. J., 5,7, (1970), 162.
7. G.C.Wood, Corros. Sci., (1962), 173.
8. J.E.Truman and K.R.Pirt, Br. Corros. J., 13,3, (1978), 136.
9. G.Betz, G.K.Weherner and L.Loeth, J. Appl. Phys., 12,45, (1974), 5312.
10. A.Kumar and D.L.Douglass, Oxid. Met., 10,1, (1976), 1.